

1 **The Genomic Formation of Human Populations in East Asia**

2

3 Chuan-Chao Wang^{1,2,3,4,*}, Hui-Yuan Yeh^{5,*}, Alexander N Popov^{6,*}, Hu-Qin
4 Zhang^{7,*}, Hirofumi Matsumura⁸, Kendra Sirak^{2,9}, Olivia Cheronet¹⁰, Alexey
5 Kovalev¹¹, Nadin Rohland², Alexander M. Kim^{2,12}, Rebecca Bernardos², Dashtseveg
6 Tumen¹³, Jing Zhao⁷, Yi-Chang Liu¹⁴, Jiun-Yu Liu¹⁵, Matthew Mah^{2,16,17}, Swapan
7 Mallick^{2,9,16,17}, Ke Wang³, Zhao Zhang², Nicole Adamski^{2,17}, Nasreen
8 Broomandkhoshbacht^{2,17}, Kimberly Callan^{2,17}, Brendan J. Culleton¹⁸, Laurie Eccles¹⁹,
9 Ann Marie Lawson^{2,17}, Megan Michel^{2,17}, Jonas Oppenheimer^{2,17}, Kristin
10 Stewardson^{2,17}, Shaoqing Wen²⁰, Shi Yan²¹, Fatma Zalzala^{2,17}, Richard Chuang¹⁴,
11 Ching-Jung Huang¹⁴, Chung-Ching Shiung¹⁴, Yuri G. Nikitin²², Andrei V. Tabarev²³,
12 Alexey A. Tishkin²⁴, Song Lin⁷, Zhou-Yong Sun²⁵, Xiao-Ming Wu⁷, Tie-Lin Yang⁷,
13 Xi Hu⁷, Liang Chen²⁶, Hua Du²⁷, Jamsranjav Bayarsaikhan²⁸, Enkhbayar Mijiddorj²⁹,
14 Diimaajav Erdenebaatar²⁹, Tumor-Ochir Iderkhangai²⁹, Erdene Myagmar¹³, Hideaki
15 Kanzawa-Kiriyama³⁰, Msato Nishino³¹, Ken-ichi Shinoda³⁰, Olga A. Shubina³²,
16 Jianxin Guo¹, Qiongying Deng³³, Longli Kang³⁴, Dawei Li³⁵, Dongna Li³⁶, Rong
17 Lin³⁶, Wangwei Cai³⁷, Rukesh Shrestha⁴, Ling-Xiang Wang⁴, Lanhai Wei¹,
18 Guangmao Xie^{38,39}, Hongbing Yao⁴⁰, Manfei Zhang⁴, Guanglin He¹, Xiaomin Yang¹,
19 Rong Hu¹, Martine Robbeets³, Stephan Schiffels³, Douglas J. Kennett⁴¹, Li Jin⁴, Hui
20 Li⁴, Johannes Krause³, Ron Pinhasi¹⁰, David Reich^{2,9,16,17}

21

- 22 1. Department of Anthropology and Ethnology, Institute of Anthropology, School of Sociology and
23 Anthropology and State Key Laboratory of Cellular Stress Biology, School of Life Sciences, Xiamen
24 University, Xiamen 361005, China
- 25 2. Department of Genetics, Harvard Medical School, Boston, Massachusetts 02115, USA
- 26 3. Max Planck Institute for the Science of Human History, 07745 Jena, Germany
- 27 4. MOE Key Laboratory of Contemporary Anthropology, Department of Anthropology and Human
28 Genetics, School of Life Sciences, Fudan University, Shanghai 200438, China
- 29 5. School of Humanities, Nanyang Technological University, Nanyang 639798, Singapore
- 30 6. Scientific Museum, Far Eastern Federal University, 690950 Vladivostok, Russia
- 31 7. Key Laboratory of Biomedical Information Engineering of Ministry of Education, School of Life
32 Science and Technology, Xi'an Jiaotong University, Xi'an 710049, China
- 33 8. School of Health Science, Sapporo Medical University, S1 W17, Chuo-ku, Sapporo, 060-8556,
34 Japan
- 35 9. Department of Human Evolutionary Biology, Harvard University, Cambridge, MA 02138, USA
- 36 10. Department of Evolutionary Anthropology, University of Vienna, 1090 Vienna, Austria
- 37 11. Institute of Archaeology, Russian Academy of Sciences, Moscow, Russia
- 38 12. Department of Anthropology, Harvard University, Cambridge, Massachusetts 02138, USA
- 39 13. Department of Anthropology and Archaeology, National University of Mongolia, Ulaanbaatar 46,
40 Mongolia
- 41 14. Institute of Archaeology, National Cheng Kung University, Tainan 701, Taiwan

- 42 15. Department of Anthropology, University of Washington, 314 Denny Hall, Seattle, USA
- 43 16. Broad Institute of Harvard and MIT, Cambridge, MA, 02142, USA
- 44 17. Howard Hughes Medical Institute, Harvard Medical School, Boston, MA 02115, USA
- 45 18. Institutes of Energy and the Environment, The Pennsylvania State University, University Park, PA
- 46 16802, USA.
- 47 19. Department of Anthropology, Pennsylvania State University, University Park, PA 16802, USA
- 48 20. Institute of Archaeological Science, Fudan University, Shanghai 200433, China
- 49 21. School of Ethnology and Sociology, Minzu University of China, Beijing 100081, China
- 50 22. Museum of Archaeology and Ethnology of Institute of History, Far Eastern Branch of Russian
- 51 Academic of Sciences, Vladivostok 690001, Russia
- 52 23. Institute of Archaeology and Ethnography, Siberian Branch of Russian Academy of Sciences,
- 53 Novosibirsk 630090, Russia
- 54 24. Department of Archeology, Ethnography and Museology, Altai State University, Barnaul, Altaysky
- 55 Kray 656049, Russia
- 56 25. Shaanxi Provincial Institute of Archaeology, Xi'an 710054, China
- 57 26. College of Cultural Heritage, Northwest University, Xi'an 710069, China
- 58 27. Xi'an AMS Center, Institute of Earth Environment, Chinese Academy of Sciences, Xi'an 710061,
- 59 China
- 60 28. Research Center at the National Museum of Mongolia, Ulaanbaatar, Region of Sukhbaatar 14201,
- 61 Mongolia
- 62 29. Department of Archaeology, Ulaanbaatar State University, Ulaanbaatar, Region of
- 63 Bayanzurkh 13343, Mongolia
- 64 30. Department of Anthropology, National Museum of Nature and Science, Tsukuba City, Ibaraki
- 65 Prefecture 305-0005, Japan
- 66 31. Archeological Center of Chiba City, Chiba 260-0814 Japan
- 67 32. Department of Archeology, Sakhalin Regional Museum, Yuzhno-Sakhalinsk, Russia
- 68 33. Department of Human Anatomy and Center for Genomics and Personalized Medicine, Guangxi
- 69 Medical University, Nanning 530021, China
- 70 34. Key Laboratory for Molecular Genetic Mechanisms and Intervention Research on High Altitude
- 71 Disease of Tibet Autonomous Region, Key Laboratory of High Altitude Environment and Gene
- 72 Related to Disease of Tibet, Ministry of Education, School of Medicine, Xizang Minzu University,
- 73 Xianyang 712082, Shaanxi, China
- 74 35. Guangxi Museum of Nationalities, Nanning 530028, Guangxi, China
- 75 36. Department of Biology, Hainan Medical University, Haikou 571199, Hainan, China
- 76 37. Department of Biochemistry and Molecular Biology, Hainan Medical University, Haikou 571199,
- 77 Hainan, China
- 78 38. College of History, Culture and Tourism, Guangxi Normal University, Guilin 541001, China
- 79 39. Guangxi Institute of Cultural Relics Protection and Archaeology, Nanning 530003, Guangxi, China
- 80 40. Belt and Road Research Center for Forensic Molecular Anthropology, Key Laboratory of Evidence
- 81 Science of Gansu Province, Gansu Institute of Political Science and Law, Lanzhou 730070, China
- 82 41. Department of Anthropology, University of California, Santa Barbara, CA 93106, USA

83
84 * Contributed equally.

85
86 Correspondence: wang@xmu.edu.cn (C-C.W), krause@shh.mpg.de (J.K.), ron.pinhasi@univie.ac.at

87 (R.P.), and reich@genetics.med.harvard.edu (D.R.).

88 **The deep population history of East Asia remains poorly understood due to a**
89 **lack of ancient DNA data and sparse sampling of present-day people. We report**
90 **genome-wide data from 191 individuals from Mongolia, northern China,**
91 **Taiwan, the Amur River Basin and Japan dating to 6000 BCE - 1000 CE, many**
92 **from contexts never previously analyzed with ancient DNA. We also report 383**
93 **present-day individuals from 46 groups mostly from the Tibetan Plateau and**
94 **southern China. We document how 6000-3600 BCE people of Mongolia and the**
95 **Amur River Basin were from populations that expanded over Northeast Asia,**
96 **likely dispersing the ancestors of Mongolic and Tungusic languages. In a time**
97 **transect of 89 Mongolians, we reveal how Yamnaya steppe pastoralist spread**
98 **from the west by 3300-2900 BCE in association with the Afanasievo culture,**
99 **although we also document a boy buried in an Afanasievo barrow with ancestry**
100 **entirely from local Mongolian hunter-gatherers, representing a unique case of**
101 **someone of entirely non-Yamnaya ancestry interred in this way. The second**
102 **spread of Yamnaya-derived ancestry came via groups that harbored about a**
103 **third of their ancestry from European farmers, which nearly completely**
104 **displaced unmixed Yamnaya-related lineages in Mongolia in the second**
105 **millennium BCE, but did not replace Afanasievo lineages in western China**
106 **where Afanasievo ancestry persisted, plausibly acting as the source of the early-**
107 **splitting Tocharian branch of Indo-European languages. Analyzing 20 Yellow**
108 **River Basin farmers dating to ~3000 BCE, we document a population that was a**
109 **plausible vector for the spread of Sino-Tibetan languages both to the Tibetan**
110 **Plateau and to the central plain where they mixed with southern agriculturalists**
111 **to form the ancestors of Han Chinese. We show that the individuals in a time**
112 **transect of 52 ancient Taiwan individuals spanning at least 1400 BCE to 600 CE**
113 **were consistent with being nearly direct descendants of Yangtze Valley first**
114 **farmers who likely spread Austronesian, Tai-Kadai and Austroasiatic languages**
115 **across Southeast and South Asia and mixing with the people they encountered,**
116 **contributing to a four-fold reduction of genetic differentiation during the**
117 **emergence of complex societies. We finally report data from Jomon hunter-**
118 **gatherers from Japan who harbored one of the earliest splitting branches of East**
119 **Eurasian variation, and show an affinity among Jomon, Amur River Basin,**
120 **ancient Taiwan, and Austronesian-speakers, as expected for ancestry if they all**
121 **had contributions from a Late Pleistocene coastal route migration to East Asia.**

122

123 **Main text**

124 East Asia, one of the oldest centers of animal and plant domestication, today harbors
125 more than a fifth of the world's human population, with present-day groups speaking

126 languages representing eleven major families: Sino-Tibetan, Tai-Kadai, Austronesian,
127 Austroasiatic, Hmong-Mien, Indo-European, Altaic (Mongolic, Turkic, and
128 Tungusic), Koreanic, Japonic, Yukghiric, and Chukotko-Kanchatkan¹. The past
129 10,000 years have been a period of profound economic and cultural change in East
130 Asia, but our current understanding of the genetic diversity, major mixture events, and
131 population movements and turnovers during the transition from foraging to
132 agriculture remains poor due to minimal sampling of the diversity of present-day
133 people on the Tibetan Plateau and southern China². A particular limitation has been a
134 deficiency in ancient DNA data, which has been a powerful tool for discerning the
135 deep history of populations in Western and Central Eurasia³⁻⁸.

136

137 We genotyped 383 present-day individuals from 46 populations indigenous to China
138 (n=337) and Nepal (n=46) using the Affymetrix Human Origins array (Table S1 and
139 Supplementary Information section 1). We also report genome-wide data from 191
140 ancient East Asians, many from cultural contexts for which there is no published
141 ancient DNA data. From Mongolia we report 89 individuals from 52 sites dating
142 between ~6000 BCE to ~1000 CE. From China we report 20 individuals from the
143 ~3000 BCE Neolithic site of Wuzhuangguoliang. From Japan we report 7 Jomon
144 hunter-gatherers from 3500-1500 BCE. From the Russian Far East we report 23
145 individuals: 18 from the Neolithic Boisman-2 cemetery at ~5000 BCE, 1 from the
146 Iron Age Yankovsky culture at ~1000 BCE, 3 from the Medieval Heishui Mohe and
147 Bohai Mohe culture at ~1000 CE; and 1 historic period hunter-gatherer from Sakhalin
148 Island. From archaeological sites in Eastern Taiwan—the Bilhun site at Hanben on the
149 main island and the Gongguan site on Green Island—we report 52 individuals from
150 the Late Neolithic through the Iron Age spanning at least 1400 BCE - 600 CE.

151

152 For all but the Chinese samples we enriched the ancient DNA for a targeted set of
153 about 1.2 million single nucleotide polymorphisms (SNPs)^{4,9}, while for the
154 Wuzhuangguoliang samples from China we used exome capture (18 individuals) or
155 shotgun sequencing (2 individuals) (Figure 1, Supplementary Data files 1 and 2 and
156 Supplementary Information section 1). We performed quality control to test for
157 contamination by other human sequences, assessed by the rate of cytosine to thymine
158 substitution in the terminal nucleotide and polymorphism in mitochondrial DNA
159 sequences¹⁰ as well as X chromosome sequences in males, and restricted analysis to

160 individuals with minimal contamination¹¹ (Online Table 1). We detected close kinship
161 between individuals at the same site, including a Boisman nuclear family with 2
162 parents and 4 children (Table S2). We merged the new data with previously reported
163 data: 4 Jomon individuals, 8 Amur River Basin Neolithic individuals from the Devil's
164 Gate site, 72 individuals from the Neolithic to the Iron Age in Southeast Asia, and 8
165 from Nepal^{7,12-20}. We assembled 123 radiocarbon dates using bone from the
166 individuals, of which 94 are newly reported (Online Table 3), and clustered
167 individuals based on time period and cultural associations, then further by genetic
168 cluster which in the Mongolian samples we designated by number (our group names
169 thus have the format “<Country>_<Time Period>_<Genetic Cluster>_<Cultural
170 Association If Any>”) (Supplementary Note, Table S1 and Online Table 1). We
171 merged the data with previously reported data (Online Table 4).

172

173 We carried out Principal Component Analysis (PCA) using smartpca²¹, projecting the
174 ancient samples onto axes computed using present-day people. The analysis shows
175 that population structure in East Asia is correlated with geographic and linguistic
176 categories, albeit with important exceptions. Groups in Northwest China, Nepal, and
177 Siberia deviate towards West Eurasians in the PCA (Supplementary Information
178 section 2, Figure 2), reflecting multiple episodes of West Eurasian-related admixture
179 that we estimate occurred 5 to 70 generations ago based on the decay of linkage
180 disequilibrium²² (Table S3 and Table S4). East Asians with minimal proportions of
181 West Eurasian-related ancestry fall along a gradient with three clusters at their poles.
182 The “Amur Basin Cluster” correlates geographically with ancient and present-day
183 populations living in the Amur River Basin, and linguistically with present-day
184 indigenous people speaking Tungusic languages and the Nivkh. The “Tibetan Plateau
185 Cluster” is most strongly represented in ancient Chokhopani, Mebrak, and Samzdong
186 individuals from Nepal¹⁵ and in present-day people speaking Tibetan-Burman
187 languages and living on the Tibetan Plateau. The “Southeast Asian Cluster” is
188 maximized in ancient Taiwan groups and present-day people in Southeast Asia and
189 southern parts of China speaking Austroasiatic, Tai-Kadai and Austronesian
190 languages (Figure S1, Figure S2). Han are intermediate among these clusters, with
191 northern Han projecting close to the Neolithic Wuzhuangguoliang individuals from
192 northern China (Figure 2). We observe two genetic clusters within Mongolia: one falls
193 closer to ancient individuals from the Amur Basin Cluster (‘East’ based on their

194 geography), and the second clusters toward ancient individuals of the Afanasievo
195 culture (‘West’), while a few individuals take intermediate positions between the two
196 (Supplementary Information section 2).

197

198 The three most ancient individuals of the Mongolia ‘East’ cluster are from the
199 Kherlen River region of eastern Mongolia (Tamsag-Bulag culture) and date to 6000-
200 4300 BCE (this places them in the Early Neolithic period, which in Northeast Asia is
201 defined by the use of pottery and not by agriculture²³). These individuals are
202 genetically similar to previously reported Neolithic individuals from the cis-Baikal
203 region and have minimal evidence of West Eurasian-related admixture as shown in
204 PCA (Figure 2), f_4 -statistics and $qpAdm$ (Table S5, Online Table 5, labeled as
205 Mongolia_East_N). The other seven Neolithic hunter-gatherers from northern
206 Mongolia (labeled as Mongolia_North_N) can be modeled as having $5.4\% \pm 1.1\%$
207 ancestry from a source related to previously reported West Siberian Hunter-gatherers
208 (WSHG)⁸ (Online Table 5), consistent with the PCA where they are part of an east-
209 west Neolithic admixture cline in Eurasia with increasing proximity to West Eurasians
210 in groups further west. Because of this ancestry complexity, we use the
211 Mongolia_East_N individuals without significant evidence of West Eurasian-related
212 admixture as reference points for modeling the East Asian-related ancestry in later
213 groups (Online Table 5). The two oldest individuals from the Mongolia ‘West’ cluster
214 have very different ancestry: they are from the Shatar Chuluu kurgan site associated
215 with the Afanasievo culture, with one directly dated to 3316-2918 calBCE (we quote
216 a 95% confidence interval here and in what follows whenever we mention a direct
217 date), and are indistinguishable in ancestry from previously published ancient
218 Afanasievo individuals from the Altai region of present-day Russia, who in turn are
219 similar to previously reported Yamnaya culture individuals supporting findings that
220 eastward Yamnaya migration had a major impact on people of the Afansievo
221 culture^{5,8}. All the later Mongolian individuals in our time transect were mixtures of
222 Mongolian Neolithic groups and more western steppe-related sources, as reflected by
223 statistics of the form f_3 (X, Y; Later Mongolian Groups), which resulted in
224 significantly negative Z scores ($Z < -3$) when Mongolia_East_N was used as X, and
225 when Yamnaya-related Steppe populations, AfontovaGora3, WSHG, or European
226 Middle/Late Neolithic or Bronze Age populations were used as Y (Table S6).

227

228 To quantify the admixture history of the later Mongolians, we again used *qpAdm*. A
229 large number of groups could be modeled as simple two-way admixtures of
230 Mongolia_East_N as one source (in proportions of 65-100%) and WSHG as the other
231 source (in proportions of 0-35%), with negligible contribution from Yamnaya-related
232 sources as confirmed by including Russia_Afanasiovo and Russia_Sintashta groups in
233 the outgroup set (Figure 3). The groups that fit this model were not only the two
234 Neolithic groups (0-5% WSHG), but also the Early Bronze Age people from the
235 Afanasievo Kurgak govi site (15%), the Ulgii group (28%), the main grouping of
236 individuals from the Middle Bronze Age Munkhkhairkhan culture (33%), Late Bronze
237 Age burials of the Ulaanzuukh type (6%), a combined group from the Center-West
238 region (27%), the Mongun Taiga type from Khukh tolgoi (35%), and people of the
239 Iron Age Slab Grave culture (9%). A striking finding in light of previous
240 archaeological and genetic data is that the male child from Kurgak govi (individual
241 I13957, skeletal code AT_629) has no evidence of Yamnaya-related ancestry despite
242 his association with Afanasievo material culture (for example, he was buried in a
243 barrow in the form of circular platform edged by vertical stone slabs, in stretched
244 position on the back on the bottom of deep rectangular pit and with a typical
245 Afanasievo egg-shaped vessel (Supplementary Note); his late Afanasievo chronology
246 is confirmed by a direct radiocarbon date of 2858-2505 BCE²⁴). This is the first
247 known case of an individual buried with Afanasievo cultural traditions who is not
248 overwhelmingly Yamnaya-related, and he also shows genetic continuity with an
249 individual buried at the same site Kurgak govi 2 in a square barrow (individual I6361,
250 skeletal code AT_635, direct radiocarbon date 2618-2487 BCE). We label this second
251 individuals as having an Ulgii cultural association, although a different archaeological
252 assessment associates this individual to the Afanasievo or Chemurchek cultures²⁵, so
253 it is possible that this provides a second example of Afanasievo material culture being
254 adopted by individuals without any Yamnaya ancestry. The legacy of the Yamnaya-
255 era spread into Mongolia continued in two individuals from the Chemurchek culture
256 whose ancestry can be only modeled by using Afanasievo as one of the sources
257 (49.0%±2.6%, Online Table 5). This model fits even when ancient European farmers
258 are included in the outgroups, showing that if the long-distance transfer of West
259 European megalithic cultural traditions to people of the Chemurchek culture that has
260 been suggested in the archaeological literature occurred,²⁶ it must have been through
261 spread of ideas rather than through movement of people.

262

263 Beginning in the Middle Bronze Age in Mongolia, there is no compelling evidence
264 for a persistence of the Yamnaya-derived lineages originally spread into the region
265 with Afanasievo. Instead in the Late Bronze Age and Iron Age and afterward we have
266 data from multiple Mongolian groups whose Yamnaya-related ancestry can only be
267 modeled as deriving not from the initial Afanasievo migration but instead from a later
268 eastward spread into Mongolia related to people of the Middle to Late Bronze Age
269 Sintashta and Andronovo horizons who were themselves a mixture of ~2/3 Yamnaya-
270 related and 1/3 European farmer-related ancestry^{5,7,8}. The Sintashta-related ancestry is
271 detected in proportions of 5% to 57% in individuals from the
272 Mongolia_LBA_6_Khovsgol (a culturally mixed group from the literature¹⁴),
273 Mongolia_LBA_3_MongunTaiga, Mongolia_LBA_5_CenterWest,
274 Mongolia_EIA_4_Sagly, Mongolia_EIA_6_Pazyryk, and Mongolia_Mongol groups,
275 with the most substantial proportions of Sintashta-related ancestry always coming
276 from western Mongolia (Figure 3, Online Table 5). For all these groups, the *qpAdm*
277 ancestry models pass when Afanasievo is included in the outgroups while models
278 with Afanasievo treated as the source with Sintashta more distantly related outgroups
279 are all rejected (Figure 3, Online Table 5). Starting from the Early Iron Age, we
280 finally detect evidence of gene flow in Mongolia from groups related to Han Chinese.
281 Specifically, when Han are included in the outgroups, our models of mixtures in
282 different proportions of Mongolia_East_N, Russia_Afanasiovo, Russia_Sintashta, and
283 WSHG continue to work for all Bronze Age and Neolithic groups, but fail for an
284 Early Iron Age individual from Tsengel sum (Mongolia_EIA_5), and for Xiongnu and
285 Mongols. When we include Han Chinese as a possible source, we estimate ancestry
286 proportions of 20-40% in Xiongnu and Mongols (Online Table 5).

287

288 While the Afanasievo-derived lineages are consistent with having largely disappeared
289 in Mongolia by the Late Bronze Age when our data showed that later groups with
290 Steppe pastoralist ancestry made an impact, we confirm and strengthen previous
291 ancient DNA analysis suggesting that the legacy of this expansion persisted in
292 western China into the Iron Age Shirezigou culture (410-190 BCE)²⁷. The only
293 parsimonious model for this group that fits according to our criteria is a 3-way
294 mixture of groups related to Mongolia_N_East, Russia_Afanasiovo, WSHG. The only
295 other remotely plausible model (although not formally a good fit) also requires

296 Russia_Afanasio as a source (Figure 3, Online Table 5). The findings of the original
297 study that reported evidence that the Afanasievo spread was the source of Steppe
298 ancestry in the Iron Age Shirengou have been questioned with the proposal of
299 alternative models that use ancient Kazakh Steppe Herders from the site of Botai,
300 Wusun, Saka and ancient Tibetans from the site of Mebrak¹⁵ in present-day Nepal as
301 major sources for Steppe and East Asian-related ancestry²⁸. However, when we fit
302 these models with Russia_Afanasio and Mongolian_East_N added to the outgroups,
303 the proposed models are rejected (P-values between 10^{-7} and 10^{-2}), except in a model
304 involving a single low coverage Saka individual from Kazakhstan as a source
305 ($P=0.17$, likely reflecting the limited power to reject models with this low coverage).
306 Repeating the modeling using other ancient Nepalese with very similar genetic
307 ancestry to that in Mebrak results in uniformly poor fits (Online Table 5). Thus,
308 ancestry typical of the Afanasievo culture and Mongolian Neolithic contributed to the
309 Shirengou individuals, supporting the theory that the Tocharian languages of the
310 Tarim Basin—from the second-oldest-known branch of the Indo-European language
311 family—spread eastward through the migration of Yamnaya steppe pastoralists to the
312 Altai Mountains and Mongolia in the guise of the Afansievo culture, from where they
313 spread further to Xinjiang^{5,7,8,27,29,30}. These results are significant for theories of Indo-
314 European language diversification, as they increase the evidence in favor of the
315 hypothesis the branch time of the second-oldest branch in the Indo-European language
316 tree occurred at the end of the fourth millennium BCE^{27,29,30}.

317

318 The individuals from the ~5000 BCE Neolithic Boisman culture and the ~1000 BCE
319 Iron Age Yankovsky culture together with the previously published ~6000 BCE data
320 from Devil's Gate cave¹⁹ are genetically very similar, documenting a continuous
321 presence of this ancestry profile in the Amur River Basin stretching back at least to
322 eight thousand years ago (Figure 2 and Figure S2). The genetic continuity is also
323 evident in the prevailing Y chromosomal haplogroup C2b-F1396 and mitochondrial
324 haplogroups D4 and C5 of the Boisman individuals, which are predominant lineages
325 in present-day Tungusic, Mongolic, and some Turkic-speakers. The Neolithic
326 Boisman individuals shared an affinity with Jomon as suggested by their intermediate
327 positions between Mongolia_East_N and Jomon in the PCA and confirmed by the
328 significantly positive statistic f_4 (Mongolia_East_N, Boisman; Mbuti, Jomon).
329 Statistics such as f_4 (Native American, Mbuti; Test East Asian,

330 Boisman/Mongolia_East_N) show that Native Americans share more alleles with
331 Boisman and Mongolia_East_N than they do with the great majority of other East
332 Asians in our dataset (Table S5). It is unlikely that these statistics are explained by
333 back-flow from Native Americans since Boisman and other East Asians share alleles
334 at an equal rate with the ~24,000-year-old Ancient North Eurasian MA1 who was
335 from a population that contributed about 1/3 of all Native American ancestry³¹. A
336 plausible explanation for this observation is that the Boisman/Mongolia Neolithic
337 ancestry was linked (deeply) to the source of the East Asian-related ancestry in Native
338 Americans^{3,31}. We can also model published data from Neolithic and Early Bronze
339 Age individuals around Lake Baikal⁷ as sharing substantial ancestry (77-94%) with
340 the lineage represented by Mongolia_East_N, revealing that this type of ancestry was
341 once spread over a wide region spanning across Lake Baikal, eastern Mongolia, and
342 the Amur River Basin (Table S7). Some present-day populations around the Amur
343 River Basin harbor large fractions of ancestry consistent with deriving from more
344 southern East Asian populations related to Han Chinese (but not necessarily Han
345 themselves) in proportions of 13-50%. We can show that this admixture occurred at
346 least by the Early Medieval period because one Heishui_Mohe individual (I3358,
347 directly dated to 1050-1220 CE) is estimated to have harbored more than 50%
348 ancestry from Han or related groups (Table S8).

349

350 The Tibetan Plateau, with an average elevation of more than 4,000 meters, is one of
351 the most extreme environments in which humans live. Archaeological evidence
352 suggests two main phases for modern human peopling of the Tibetan Plateau. The
353 first can be traced back to at least ~160,000 years ago probably by Denisovans³² and
354 then to 40,000-30,000 years ago as reflected in abundant blade tool assemblages³³.
355 However, it is only in the last ~3,600 years that there is evidence for continuous
356 permanent occupation of this region with the advent of agriculture³⁴. We grouped 17
357 present-day populations from the highlands into three categories based on genetic
358 clustering patterns (Figure S3): “Core Tibetans” who are closely related to the ancient
359 Nepal individuals such as Chokopani with a minimal amount of admixture with
360 groups related to West Eurasians and lowland East Asians in the last dozens of
361 generations, “northern Tibetans” who are admixed between lineages related to Core
362 Tibetans and West Eurasians, and “Tibeto-Yi Corridor” populations (the eastern edge
363 of the Tibetan Plateau connecting the highlands to the lowlands) that includes not just

364 Tibetan speakers but also Qiang and Lolo-Burmese speakers who we estimate using
365 $qpAdm^{4,35}$ have 30-70% Southeast Asian Cluster-related ancestry (Table S9). We
366 computed f_3 (Mbuti; Core Tibetan, non-Tibetan East Asian) to search for non-Tibetans
367 that share the most genetic drift with Tibetans. Neolithic Wuzhuangguoliang, Han and
368 Qiang appear at the top of the list (Table S10), suggesting that Tibetans harbor
369 ancestry from a population closely related to Wuzhuangguoliang that also contributed
370 more to Qiang and Han than to other present-day East Asian groups. We estimate that
371 the mixture occurred 60-80 generations ago (2240-1680 years ago assuming 28 years
372 per generation³⁶ under a model of a single pulse of admixture (Table S11). This
373 represents an average date and so only provides a lower bound on when these two
374 populations began to mix; the start of their period of admixture could plausibly be as
375 old as the ~3,600-year-old date for the spread of agriculture onto the Tibetan plateau.
376 These findings are therefore consistent with archaeological evidence that expansions
377 of farmers from the Upper and Middle Yellow River Basin influenced populations of
378 the Tibetan Plateau from the Neolithic to the Bronze Age as they spread across the
379 China Central plain^{37,38}, and with Y chromosome evidence that the shared common
380 haplogroup O α -F5 between Han and Tibetans coalesced to a common ancestry less
381 than 5,800 years ago³⁹.

382

383 In the south, we find that the ancient Taiwan Hanben and Gongguan culture
384 individuals dating from at least a span of 1400 BCE - 600 CE are genetically most
385 similar to present-day Austronesian speakers and ancient Lapita individuals from
386 Vanuatu as shown in outgroup f_3 -statistics and significantly positive f_4 -statistics
387 (Taiwan_Hanben/Gongguan, Mbuti; Ami/Atayal/Lapita, other Asians) (Table S8).
388 The similarity to Austronesian-speakers is also evident in the Iron Age dominant
389 paternal Y chromosome lineage O3a2c2-N6 and maternal mtDNA lineages E1a,
390 B4a1a, F3b1, and F4b, which are widespread lineages among Austronesian-
391 speakers^{40,41}. We compared the present-day Austronesian-speaking Ami and Atayal of
392 Taiwan with diverse Asian populations using statistics like f_4 (Taiwan Iron
393 Age/Austronesian, Mbuti; Asian1, Asian2). Ancient Taiwan groups and Austronesian-
394 speakers share significantly more alleles with Tai-Kadai speakers in southern
395 mainland China and in Hainan Island⁴² than they do with other East Asians (Table
396 S8), consistent with the hypothesis that ancient populations related to present-day Tai-
397 Kadai speakers are the source for the spread of agriculture to Taiwan island around

398 5000 years ago⁴³. The Jomon share alleles at an elevated rate with ancient Taiwan
399 individuals and Ami/Atayal as measured by statistics of the form f_4 (Jomon, Mbuti;
400 Ancient Taiwan/Austronesian-speaker, other Asians) compared with other East Asian
401 groups, with the exception of groups in the Amur Basin Cluster (Table S8)⁴⁴.

402

403 The Han Chinese are the world's largest ethnic group. It has been hypothesized based
404 on the archaeologically documented spread of material culture and farming
405 technology, as well as the linguistic evidence of links among Sino-Tibetan languages,
406 that one of the ancestral populations of the Han might have consisted of early farmers
407 along the Upper and Middle Yellow River in northern China, some of whose
408 descendants also may have spread to the Tibetan Plateau and contributed to present-
409 day Tibeto-Burmans⁴⁵. Archaeological and historical evidence document how during
410 the past two millennia, the Han expanded south into regions inhabited by previously
411 established agriculturalists⁴⁶. Analysis of genome-wide variation among present-day
412 populations has revealed that the Han Chinese are characterized by a “North-South”
413 cline^{47,48}, which is confirmed by our analysis. The Neolithic Wuzhuangguoliang,
414 present-day Tibetans, and Amur River Basin populations, share significantly more
415 alleles with Han Chinese compared with the Southeast Asian Cluster, while the
416 Southeast Asian Cluster groups share significantly more alleles with the majority of
417 Han Chinese groups when compared with the Neolithic Wuzhuangguoliang (Table
418 S12, Table S13). These findings suggest that Han Chinese may be admixed in variable
419 proportions between groups related to Neolithic Wuzhuangguoliang and people
420 related to those of the Southeast Asian Cluster. To determine the minimum number of
421 source populations needed to explain the ancestry of the Han, we used *qpWave*^{4,49} to
422 study the matrix of all possible statistics of the form f_4 (Han₁, Han₂; O₁, O₂), where
423 “O₁” and “O₂” are outgroups that are unlikely to have been affected by recent gene
424 flow from Han Chinese. This analysis confirms that two source populations are
425 consistent with all of the ancestry in most Han Chinese groups (with the exception of
426 some West Eurasian-related admixture that affects some northern Han Chinese in
427 proportions of 2-4% among the groups we sampled; Table S14 and Table S15).
428 Specifically, we can model almost all present-day Han Chinese as mixtures of two
429 ancestral populations, in a variety of proportions, with 77-93% related to Neolithic
430 Wuzhuangguoliang from the Yellow River basin, and the remainder from a
431 population related to ancient Taiwan that we hypothesize was closely related to the

432 rice farmers of the Yangtze River Basin. This is also consistent with our inference that
433 the Yangtze River farmer related ancestry contributed nearly all the ancestry of
434 Austronesian speakers and Tai-Kadai speakers and about 2/3 of some Austroasiatic
435 speakers^{17,20} (Figure 4). A caveat is that there is a modest level of modern
436 contamination in the Wuzhuangguoliang we use as a source population for this
437 analysis (Online Table 1), but this would not bias admixture estimates by more than
438 the contamination estimate of 3-4%. The average dates of West Eurasian-related
439 admixture in northern Han Chinese populations Han_NChina and Han_Shanxi are 32-
440 45 generations ago, suggesting that mixture was continuing at the time of the Tang
441 Dynasty (618-907 CE) and Song Dynasty (960-1279 BCE) during which time there
442 are historical records of integration of Han Chinese and western ethnic groups, but
443 this date is an average so the mixture between groups could have begun earlier.

444
445 To obtain insight into the formation of present-day Japanese archipelago populations,
446 we searched for groups that contribute most strongly to present-day Japanese through
447 admixture f_3 -statistics. The most strongly negative signals come from mixtures of Han
448 Chinese and ancient Jomon ($f_3(\text{Japanese}; \text{Han Chinese, Jomon})$) (Table S16). We can
449 model present-day Japanese as two-way mixtures of 84.3% Han Chinese and 15.7%
450 Jomon or 87.6% Korean and 12.4% Jomon (we cannot distinguish statistically
451 between these two sources; Table S17 and Table S18). This analysis by no means
452 suggests that the mainland ancestry in Japan was contributed directly by the Han
453 Chinese or Koreans themselves, but does suggest that it is from an ancestral
454 population related to those that contributed in large proportion to Han Chinese as well
455 as to Koreans for which we do not yet have ancient DNA data.

456
457 We used *qpGraph*³⁵ to explore models with population splits and gene flow, and
458 tested their fit to the data by computing f_2 -, f_3 - and f_4 - statistics measuring allele
459 sharing among pairs, triples, and quadruples of populations, evaluating fit based on
460 the maximum $|Z|$ -score comparing predicted and observed values. We further
461 constrained the models by using estimates of the relative population split times
462 between the selected pairs of populations based on the output of the MSMC
463 software⁵⁰. While admixture graph modeling based on allele frequency correlation
464 statistics is not able to reject a model in which ancient Taiwan individuals and
465 Boismans share substantial ancestry with each other more recently than either does

466 with the ancestors of Chokopani and Core Tibetans, this model cannot be correct
467 because our MSMC analysis reveals that Core Tibetans (closely related to Chokopani)
468 and Ulchi (closely related to Boisman) share ancestry more recently in time on
469 average than either does with Ami (related to Taiwan_Hanben). This MSMC-based
470 constraint allowed us to identify a parsimonious working model for the deep history
471 of key lineages discussed in this study (Supplementary Information section 3:
472 *qpGraph* Modeling). Our fitted model (Figure 5), suggests that much of East Asian
473 ancestry today can be modelled as derived from two ancient populations: one from the
474 same lineage as the approximately ~40,000-year-old Tianyuan individual and the
475 other more closely related to Onge, with groups today having variable proportions of
476 ancestry from these two deep sources. In this model, the Mongolia_East_N and Amur
477 River Basin Boisman related lineages derive the largest proportion of their ancestry
478 from the Tianyuan-related lineage and the least proportion of ancestry from the Onge-
479 related lineage compared with other East Asians. A sister lineage of
480 Mongolia_East_N is consistent with expanding into the Tibetan Plateau and mixing
481 with the local hunter-gatherers who represent an Onge-related branch in the tree. The
482 Taiwan Hanben are well modelled as deriving about 14% of their ancestry from a
483 lineage remotely related to Onge and the rest of their ancestry from a lineage that also
484 contributed to Jomon and Boisman on the Tianyuan side, a scenario that would
485 explain the observed affinity among Jomon, Boisman and Taiwan Hanben. We
486 estimate that Jomon individuals derived 45% of their ancestry from a deep basal
487 lineage on the Onge side. These results are consistent with the scenario a Late
488 Pleistocene coastal route of human migration linking Southeast Asia, the Japanese
489 Archipelago and the Russian Far East⁵¹. Due to the paucity of ancient genomic data
490 from Upper Paleolithic East Asians, there are limited constraints at present for
491 reconstructing the deep branching patterns of East Asian ancestral populations, and it
492 is certain that this admixture graph is an oversimplification and that additional
493 features of deep population relationships will be revealed through future work.

494

495 At the end of the last Ice Age, there were multiple highly differentiated populations in
496 East as well as West Eurasia, and it is now clear that these groups mixed in both
497 regions, instead of one population displacing the others. In West Eurasia, there were
498 at least four divergent populations each as genetically differentiated from each other
499 as Europeans and East Asians today (average $F_{ST}=0.10$), which mixed in the

500 Neolithic, reducing heterogeneity (average $F_{ST}=0.03$) and mixed further in the Bronze
501 Age and Iron Age to produce the present-relatively low differentiation that
502 characterizes modern West Eurasia (average $F_{ST}=0.01$)⁵². In East Eurasia, our study
503 suggests an analogous process, with the differentiation characteristic of the Amur
504 River Basin groups, Neolithic Yellow River farmers, and people related to those of
505 the Taiwan Iron Age (average $F_{ST}=0.06$ in our data) collapsing through mixture to
506 today's relatively low differentiation (average $F_{ST}=0.01-0.02$) (Figure 6). A priority
507 should be to obtain ancient DNA data for the hypothesized Yangtze River population
508 (the putative source for the ancestry prevalent in the Southeast Asian Cluster of
509 present-day groups), which should, in turn, make it possible to test and further extend
510 these models, and in particular to understand if dispersals of people in Southeast Asia
511 do or do not correlate to ancient movements of people.

512 **References**

- 513 1. Cavalli-Sforza, L. L. The Chinese human genome diversity project. *Proc. Natl. Acad. Sci.*
514 *USA* **95**, 11501-11503 (1998).
- 515 2. HUGO Pan-Asian SNP Consortium. Mapping human genetic diversity in Asia. *Science* **326**,
516 1541-1545 (2009).
- 517 3. Lazaridis, I., et al. Ancient human genomes suggest three ancestral populations for present-
518 day Europeans. *Nature* **513**, 409-413 (2014).
- 519 4. Haak, W., et al. Massive migration from the steppe was a source for Indo-European languages
520 in Europe. *Nature* **522**, 207–211 (2015).
- 521 5. Allentoft, M.E., et al.. Population genomics of Bronze Age Eurasia. *Nature* **522**,167-172
522 (2015).
- 523 6. Fu, Q., et al.. The genetic history of ice age Europe. *Nature* **534**, 200-205 (2016).
- 524 7. de Barros Damgaard, P., et al.. 137 ancient human genomes from across the Eurasian steppes.
525 *Nature* **557**, 369-374 (2018).
- 526 8. Narasimhan, V.M., et al. The formation of human populations in South and Central Asia.
527 *Science* **365**, eaat7487 (2019).
- 528 9. Fu, Q., et al. An early modern human from Romania with a recent Neanderthal ancestor.
529 *Nature* **524**, 216–219 (2015).
- 530 10. Fu, Q., et al. DNA analysis of an early modern human from Tianyuan Cave, China. *Proc. Natl*
531 *Acad. Sci. USA* **110**, 2223–2227 (2013).
- 532 11. Korneliussen, T. S., Albrechtsen, A., & Nielsen, R. ANGSD: Analysis of Next Generation
533 Sequencing Data. *BMC Bioinformatics* **15**, 356 (2014).
- 534 12. Posth, C., et al. Language continuity despite population replacement in Remote Oceania. *Nat*
535 *Ecol Evol.* **2**, 731-740 (2018).
- 536 13. Sikora, M., et al. The population history of northeastern Siberia since the Pleistocene. *Nature*
537 **570**, 182-188 (2019).
- 538 14. Jeong, C., et al. The genetic history of admixture across inner Eurasia. *Nat. Ecol. Evol.* **3**,
539 966–976 (2019).
- 540 15. Jeong, C., et al. Long-term genetic stability and a high-altitude East Asian origin for the
541 peoples of the high valleys of the Himalayan arc. *Proc. Natl. Acad. Sci. USA* **113**, 7485–7490
542 (2016).
- 543 16. Skoglund, P., et al. Genomic insights into the peopling of the Southwest Pacific. *Nature* **538**,
544 510-513 (2016).
- 545 17. Lipson, M., et al. Ancient genomes document multiple waves of migration in Southeast Asian
546 prehistory. *Science* **361**, 92-95 (2018).
- 547 18. Kanzawa-Kiriyama, H., et al. A partial nuclear genome of the Jomons who lived 3000 years
548 ago in Fukushima, Japan. *J. Hum. Genet* **62**, 213–221 (2016).

- 549 19. Siska, V., et al. Genome-wide data from two early Neolithic East Asian individuals dating to
550 7700 years ago. *Sci Adv.* **3**, e1601877 (2017).
- 551 20. McColl, H., et al. The prehistoric peopling of Southeast Asia. *Science*. **361**, 88-92 (2018).
- 552 21. Patterson, N., Price, A. L., & Reich, D. Population structure and eigenanalysis. *PLoS Genet.* **2**,
553 e190 (2006).
- 554 22. Loh, P.R., et al. Inferring admixture histories of human populations using linkage
555 disequilibrium. *Genetics* **193**, 1233-1254 (2013).
- 556 23. Jordan, P. & Zvelebil M. ed. *Ceramics Before Farming: The Dispersal of Pottery Among*
557 *Prehistoric Eurasian Hunter-Gatherers* (Routledge, New York, 2010).
- 558 24. Kovalev, A. A., & Erdenebaatar, D. Discovery of New Cultures of the Bronze Age in
559 Mongolia according to the Data obtained by the International Central Asian Archaeological
560 Expedition. In *Current Archaeological Research in Mongolia*, (eds Bemmann, J., H.
561 Parzinger, H., Pohl, E., D. Tseveendorzh, D.) 149–170 (Bonn: Vor- und Frühgeschichtliche
562 Archäologie Rheinische Friedrich-Wilhelm-Universität Bonn, 2009).
- 563 25. Wilkins, S., et al. Dairy pastoralism sustained eastern Eurasian steppe populations for 5,000
564 years. *Nat Ecol Evol* **4**, 346–355 (2020).
- 565 26. Kovalev, A. The Great Migration of the Chemurchek People from France to the Altai in the
566 Early 3rd Millennium BCE. *International Journal of Eurasian Studies*. 1(11), pp. 1-58
567 (2011).
- 568 27. Ning, C., et al. Ancient Genomes Reveal Yamnaya-Related Ancestry and a Potential Source of
569 Indo-European Speakers in Iron Age Tianshan. *Curr Biol.* **29**, 2526-2532.e4 (2019).
- 570 28. Weslowski. Eurogenes Blog: A surprising twist to the Shirezigou nomads story
571 (2019).<https://eurogenes.blogspot.com/2019/08/a-surprising-twist-to-shirezigou.html>.
- 572 29. Mallory, J.P. *In Search of the INDO-Europeans: Language, Archaeology and Myth* (Thames &
573 Hudson, New York, 1991).
- 574 30. Anthony, D. *The Horse, the Wheel, and Language: How Bronze-Age Riders from the Eurasian*
575 *Steppes Shaped the Modern World* (Princeton University Press, Princeton and Oxford, 2007).
- 576 31. Raghavan, M., et al. Upper Palaeolithic Siberian genome reveals dual ancestry of Native
577 Americans. *Nature* **505**, 87-91 (2014).
- 578 32. Chen, F., et al. A late Middle Pleistocene Denisovan mandible from the Tibetan Plateau.
579 *Nature* **569**, 409-412 (2019).
- 580 33. Zhang, X. L., et al. The earliest human occupation of the high-altitude Tibetan Plateau 40
581 thousand to 30 thousand years ago. *Science* **362**, 1049-1051 (2018).
- 582 34. Chen, F.H., et al. Agriculture facilitated permanent human occupation of the Tibetan Plateau
583 after 3600 B.P. *Science* **347**, 248-250 (2015).
- 584 35. Patterson, N., et al. Ancient admixture in human history. *Genetics* **192**, 1065-1093 (2012).

- 585 36. Moorjani, M., Sankararaman, S., Fu, Q., Przeworski, M., Patterson, N., & Reich, D. A genetic
586 method for dating ancient genomes provides a direct estimate of human generation interval in
587 the last 45,000 years. *Proc. Natl. Acad. Sci. USA* **113**, 5652-5657 (2016).
- 588 37. Barton, L., et al. Agricultural origins and the isotopic identity of domestication in northern
589 China. *Proc. Natl. Acad. Sci. USA* **106**, 5523-5528 (2009).
- 590 38. Yang, X., et al. Early millet use in northern China. *Proc. Natl. Acad. Sci. USA* **109**, 3726–3730
591 (2012).
- 592 39. Wang, L.X., et al. Reconstruction of Y-chromosome phylogeny reveals two neolithic
593 expansions of Tibeto-Burman populations. *Mol Genet Genomics*. **293**, 1293-1300 (2018).
- 594 40. Wei, L.H., et al. Phylogeography of Y-chromosome haplogroup O3a2b2-N6 reveals patrilineal
595 traces of Austronesian populations on the eastern coastal regions of Asia. *PLoS One* **12**,
596 e0175080 (2017).
- 597 41. Ko, A.M., et al. Early Austronesians: into and out of Taiwan. *Am. J. Hum. Genet.* **94**, 426-36
598 (2014).
- 599 42. Lipson, M., et al. Reconstructing Austronesian population history in island Southeast Asia.
600 *Nat Commun.* **5**, 4689 (2014).
- 601 43. Bellwood, P. The checkered prehistory of rice movement southwards as a domesticated
602 cereal—from the Yangzi to the equator. *Rice* **4**, 93-103 (2011).
- 603 44. Kanzawa-Kiriyama H., et al. Late Jomon male and female genome sequences from the
604 Funadomari site in Hokkaido, Japan. *Anthropol Sci.* **127**, 83-108 (2019).
- 605 45. Su, B., et al. Y chromosome haplotypes reveal prehistorical migrations to the Himalayas.
606 *Hum. Genet.* **107**, 582-590 (2000).
- 607 46. Ge, J. X., Wu, S. D., & Chao, S. J. *Zhongguo yimin shi (The Migration History of China)*
608 (Fujian People's Publishing House, Fuzhou, 1997).
- 609 47. Chen, J., et al. Genetic structure of the Han Chinese population revealed by genome-wide
610 SNP variation. *Am. J. Hum. Genet.* **85**, 775-785 (2009).
- 611 48. Xu, S., et al. Genomic dissection of population substructure of Han Chinese and its
612 implication in association studies. *Am. J. Hum. Genet.* **85**, 762-774 (2009).
- 613 49. Reich, D., et al. Reconstructing Native American population history. *Nature* **488**, 370-374
614 (2012).
- 615 50. Schiffels, S., & Durbin, R. Inferring human population size and separation history from
616 multiple genome sequences. *Nat Genet.* **46**, 919-925 (2014).
- 617 51. Matsumura, H., et al. Craniometrics Reveal "Two Layers" of Prehistoric Human Dispersal in
618 Eastern Eurasia. *Sci Rep.* **9**, 1451 (2019).
- 619 52. Lazaridis, I., et al. Genomic insights into the origin of farming in the ancient Near East.
620 *Nature* **536**, 419–424 (2016).
- 621
622

623 **Methods**

624 **Ancient DNA laboratory work**

625 All samples except those from Wuzhuangguoliang were prepared in dedicated clean
626 room facilities at Harvard Medical School, Boston, USA. Online Table 2 lists
627 experimental settings for each sample and library included in the dataset. Skeletal
628 samples were surface cleaned and drilled or sandblasted and milled to produce a fine
629 powder for DNA extraction^{53,54}. We then either followed the extraction protocol by
630 Dabney et al⁵⁵ replacing the extender-MinElute-column assembly with the columns
631 from the Roche High Pure Viral Nucleic Acid Large Volume Kit⁵⁶ (manual
632 extraction) or, for samples prepared later, used DNA extraction protocol based on
633 silica beads instead of spin columns (and Dabney buffer) to allow for automated DNA
634 purification⁵⁷ (robotic extraction). We prepared individually barcoded double-
635 stranded libraries for most samples using a protocol that included a DNA repair step
636 with Uracil-DNA-glycosylase (UDG) treatment to cut molecules at locations
637 containing ancient DNA damage that is inefficient at the terminal positions of DNA
638 molecules (Online Table 1, UDG: “half”)⁵⁸, or, without UDG pre-treatment (double
639 stranded minus). For a few samples processed later, single stranded DNA libraries⁵⁹
640 were prepared with USER (NEB) addition in the dephosphorylation step that results
641 in inefficient uracil removal at the 5’ end of the DNA molecules, and does not affect
642 deamination rates at the terminal 3’ end⁶⁰. We performed target enrichment via
643 hybridization of these libraries with previously reported protocols¹⁰. We either
644 enriched for the mitochondrial genome and 1.2M SNPs in two separate experiments
645 or together in a single experiment. If split over two experiments, the first enrichment
646 was for sequences aligning to mitochondrial DNA^{58,61} with some baits overlapping
647 nuclear targets spiked in to screen libraries for nuclear DNA content. The second in-
648 solution enrichment was for a targeted set of 1,237,207 SNPs that comprises a merge
649 of two previously reported sets of 394,577 SNPs (390k capture)⁴ and 842,630 SNPs⁹.
650 We sequenced the enriched libraries on an Illumina NextSeq500 instrument for 2x76
651 cycles (and both indices) or on Hiseq X10 instruments at the Broad Institute of MIT
652 and Harvard for 2x101 cycles. We also shotgun sequenced each library for a few
653 hundred thousand reads to assess the fraction of human reads.

654

655 Ancient DNA extractions of the Wuzhuangguoliang samples were performed in the
656 clean room at Xi'an Jiaotong University and Xiamen University following the

657 protocol by Rohland and Hofreiter⁶². Each sample extract was converted into double-
658 stranded Illumina libraries following the manufacturer's protocol (Fast Library Prep
659 Kit, iGeneTech, Beijing, China). Sample-specific indexing barcodes were added to
660 both sides of the fragments via amplification. Nuclear DNA capture was performed
661 with AIExome Enrichment Kit V1 (iGeneTech, Beijing, China) according to the
662 manufacturer's protocol and sequenced on an Illumina NovaSeq instrument with 150
663 base pair paired-end reads. Sequences that did not perfectly match one of the expected
664 index combinations were discarded.

665

666 For the AH1-7 and AH1-17 DNA extracts, we prepared whole genome sequencing
667 libraries. The two DNA extracts were converted into barcoded Illumina sequencing
668 libraries using commercially available library kits (NEBNext[®] Ultra[™] II DNA
669 Library Prep Kit) and Illumina-specific primers⁶³. DNA libraries were not treated with
670 uracil-DNA-glycosylase (UDG)⁵⁹. We used a MinElute Gel Extraction Kit (Qiagen,
671 Hilden, Germany) for purification. Two libraries were sequenced on a HiSeqX10
672 instrument (2×150 bp, PE) at the Novogene Sequencing Centre (Beijing, China). The
673 base calling was performed using CASAVA software.

674

675 **Bioinformatic processing**

676 For the sequencing data produced at Harvard Medical School, we used one of two
677 pipelines ("pipeline 1" or "pipeline 2"; Online Table 2). An up-to-date description of
678 both pipelines and analyses showing that the differences between them do not cause
679 systematic bias in population genetic analysis can be found in Fernandes et al⁶⁴. For
680 both pipelines we began by de-multiplexed the data and assigning sequences to
681 samples based on the barcodes and/or indices, allowing up to one mismatch per
682 barcode or index. We trimmed adapters and restricted to fragments where the two
683 reads overlapped by at least 15 nucleotides. In pipeline 1 we merged the sequences
684 (allowing up to one mismatch) using a modified version of *Seqprep*⁶⁵ where bases in
685 the merged region are chosen based on highest quality in case of a conflict, and in
686 pipeline 2 we used custom software (<https://github.com/DReichLab/ADNA-Tools>).
687 For mitochondrial DNA analysis, we aligned the resulting merged sequences to the
688 RSRS reference genome⁶⁶ using *bwa* (version 0.6.1 for pipeline 1 and version 0.7.15
689 for pipeline 2)⁶⁷, and removed duplicates with the same orientation, start and stop
690 positions, and molecular barcodes. We determined mitochondrial DNA haplogroups

691 using *HaploGrep2*⁶⁸. We also analyzed the sequences to generate two assessments of
692 ancient DNA authenticity. The first assessment estimated the rate of cytosine to
693 thymine substitution in the final nucleotide, which is expected to be at least 3% at
694 cytosines in libraries prepared with a partial UDG treatment protocol and at least 10%
695 for untreated libraries (minus) and single stranded libraries; all libraries we analyzed
696 met this threshold. The second assessment used *contamMix* (version 1.0.9 for pipeline
697 1 and 1.0.12 for pipeline 2)¹⁰ to determine the fraction of mtDNA sequences in an
698 ancient sample that match the endogenous majority consensus more closely than a
699 comparison set of 311 worldwide present-day human mtDNAs (Online Table 1).
700 Computational processing of the sequence data from the whole genome was the same
701 as the mtDNA enrichment except that the human genome (hg19) was used as the
702 target reference. Due to the low coverage, diploid calling was not possible; instead,
703 we randomly selected a single sequence covering every SNP position of interest
704 (“pseudo-haploid” data) using custom software, only using nucleotides that were a
705 minimum distance from the ends of the sequences to avoid deamination artifacts
706 (<https://github.com/DReichLab/adna-workflow>). The coverages and numbers of SNPs
707 covered at least once on the autosomes (chromosomes 1-22) are in Online Table 1.

708

709 For the sequencing data from the Wuzhuangguoliang samples, we clipped adaptors
710 with *leehom*⁶⁹ and then further processed using *EAGER*⁷⁰, including mapping with
711 *bwa* (v0.6.1)⁶⁷ against the human genome reference GRCh37/hg19 (or just the
712 mitochondrial reference sequence), and removing duplicate reads with the same
713 orientation and start and end positions. To avoid an excess of remaining C-to-T and
714 G-to-A transitions at the ends of the sequences, we clipped three bases of the ends of
715 each read for each sample using *trimBam*
716 (https://genome.sph.umich.edu/wiki/BamUtil:_trimBam). We generated pseudo-
717 haploid calls by selecting a single read randomly for each individual using
718 *pileupCaller* (<https://github.com/stschiff/sequenceTools/tree/master/srcpileupCaller>).

719

720 **Accelerator Mass Spectrometry Radiocarbon Dating**

721 We generated 94 direct AMS (Accelerator Mass Spectrometry) radiocarbon (¹⁴C)
722 dates as part of this study; 87 at Pennsylvania State University (PSU) and 7 at Poznan
723 Radiocarbon Laboratory. The methods used at both laboratories are published, and
724 here we summarize the methods from PSU. Bone collagen from petrous, phalanx, or

725 tooth (dentine) samples was extracted and purified using a modified Longin method
726 with ultrafiltration (>30kDa gelatin)⁷¹. If bone collagen was poorly preserved or
727 contaminated we hydrolyzed the collagen and purified the amino acids using solid
728 phase extraction columns (XAD amino acids)⁷². Prior to extraction we sequentially
729 sonicated all samples in ACS grade methanol, acetone, and dichloromethane (30
730 minutes each) at room temperature to remove conservants or adhesives possibly used
731 during curation. Extracted collagen or amino acid preservation was evaluated using
732 crude gelatin yields (% wt), %C, %N and C/N ratios. Stable carbon and nitrogen
733 isotopes were measured on a Thermo DeltaPlus instrument with a Costech elemental
734 analyzer at Yale University. C/N ratios between 3.14 and 3.45 indicate that all
735 radiocarbon dated samples are well preserved. All samples were combusted and
736 graphitized at PSU using methods described in Kennett et al. 2017⁷¹. ¹⁴C
737 measurements were made on a modified National Electronics Corporation 1.5SDH-1
738 compact accelerator mass spectrometer at either the PSUAMS facility or the Keck-
739 Carbon Cycle AMS Facility. All dates were calibrated using the IntCal13 curve⁷³ in
740 OxCal v 4.3.2⁷⁴ and are presented in calendar years BCE/CE .

741

742 **Y chromosomal haplogroup analysis**

743 We performed Y-haplogroup determination by examining the state of SNPs present in
744 ISOGG version 11.89 (accessed March 31, 2016) and our unpublished updated
745 phylogeny.

746

747 **X-chromosome contamination estimates**

748 We performed an X-chromosomal contamination test for the male individuals
749 following an approach introduced by Rasmussen et al⁷⁵ and implemented in the
750 *ANGSD* software suite¹¹. We used the “MoM” (Methods of Moments) estimates. The
751 estimates for some males are not informative because of the limited number of X-
752 chromosomal SNPs covered by at least two sequences, and hence we only report
753 results for individuals with at least 200 SNPs covered at least twice. The estimated
754 contamination rates for the male samples are low (Online Table 1). The contamination
755 rates for all samples are quite low except those from Wuzhuangguoliang. We detected
756 3-6% contamination in the Wuzhuangguoliang samples, and restricted population
757 genetic modeling analysis only to three males with 3-4% contamination.

758

759 **Data merging**

760 We merged the data with previously published datasets genotyped on Affymetrix
761 Human Origins arrays^{3,35}, restricting to individuals with >95% genotyping
762 completeness. We manually curated the data using ADMIXTURE⁷⁶ and
763 EIGENSOFT²¹ to identify samples that were outliers compared with other samples
764 from their own populations. We removed seven individuals from subsequent analysis;
765 the population IDs for these individuals are prefixed by the string “Ignore_” in the
766 dataset we release, so users who wish to analyze these samples are still able to do so.

767

768 **Principal Components Analysis.** We carried out principal components analysis in
769 the *smartpca* program of EIGENSOFT²¹, using default parameters and the `lsqproject:`
770 `YES` and `numoutlieriter: 0` options.

771

772 **ADMIXTURE Analysis.** We carried out ADMIXTURE analysis in unsupervised
773 mode⁷⁶ after pruning for linkage disequilibrium in PLINK⁷⁷ with parameters `--indep-`
774 `pairwise 200 25 0.4` which retained 256,427 SNPs for Human Origin Dataset. We ran
775 ADMIXTURE with default 5-fold cross-validation (`--cv=5`), varying the number of
776 ancestral populations between $K=2$ and $K=18$ in 100 bootstraps with different random
777 seeds.

778

779 ***f*-statistics.** We computed f_3 -statistics and f_4 -statistics using ADMIXTOOLS³⁵ with
780 default parameters. We computed standard errors using a block jackknife⁷⁸.

781

782 **F_{ST} computation.** We estimated F_{ST} using EIGENSOFT²¹ with default parameters,
783 `inbreed: YES`, and `fstonly: YES`. We found that the inbreeding corrected and
784 uncorrected F_{ST} were nearly identical (within ~ 0.001), and in this study, always
785 analyzed uncorrected F_{ST} .

786

787 **Admixture graph modeling.** Admixture graph modeling was carried out with the
788 *qpGraph* software as implemented in ADMIXTOOLS³⁵ using Mbuti as an outgroup.

789

790 **Testing for the number of streams of ancestry.** We used *qpWave*^{4,35} as
791 implemented in ADMIXTOOLS to test whether a set of test populations is consistent
792 with being related via N streams of ancestry from a set of outgroup populations.

793

794 **Inferring mixture proportions without an explicit phylogeny.** We used *qpAdm*⁴ as
795 implemented in ADMIXTOOLS to estimate mixture proportions for a *Test* population
796 as a combination of *N* ‘reference’ populations by exploiting (but not explicitly
797 modeling) shared genetic drift with a set of ‘Outgroup’ populations.

798

799 **Weighted linkage disequilibrium (LD) analysis.** LD decay was calculated using
800 ALDER²² to infer admixture parameters including dates and mixture proportions.

801

802 **MSMC.** We used MSMC⁵⁰ following the procedures in Mallick et al⁷⁹ to infer cross-
803 coalescence rates and population sizes among Ami/Atayal, Tibetan, and Ulchi.

804

805 **Kinship analysis.** We used READ software⁸⁰ as well as a custom method⁸¹ to
806 determine genetic kinship between individual pairs.

807

808 **Data availability**

809 The aligned sequences are available through the European Nucleotide Archive under
810 accession number [to be made available on publication]. Genotype data used in
811 analysis are available at <https://reich.hms.harvard.edu/datasets>. Any other relevant
812 data are available from the corresponding author upon reasonable request.

813

- 814 53. Pinhasi, R., Fernandes, D.M., Sirak, K., & Cheronet, O. Isolating the human cochlea to
815 generate bone powder for ancient DNA analysis. *Nat Protoc.* **14**, 1194-1205 (2019).
- 816 54. Sirak, K.A., et al., A minimally-invasive method for sampling human petrous bones from the
817 cranial base for ancient DNA analysis. *Biotechniques.* **62**, 283-289 (2017).
- 818 55. Dabney, J., et al. Complete mitochondrial genome sequence of a Middle Pleistocene cave bear
819 reconstructed from ultrashort DNA fragments. *Proc Natl Acad Sci U S A.* **110**, 15758-63
820 (2013).
- 821 56. Korlević, P. Reducing microbial and human contamination in DNA extractions from ancient
822 bones and teeth. *Biotechniques.* **59**, 87-93 (2015).
- 823 57. Rohland, N., Glocke, I., Aximu-Petri, A., & Meyer, M. Extraction of highly degraded DNA
824 from ancient bones, teeth and sediments for high-throughput sequencing. *Nat Protoc.* **13**,
825 2447-2461 (2018).

- 826 58. Rohland, N., Harney, E., Mallick, S., Nordenfelt, S. & Reich, D. Partial uracil–DNA–
827 glycosylase treatment for screening of ancient DNA. *Phil. Trans. R. Soc. Lond. B* **370**,
828 20130624 (2015).
- 829 59. Gansauge, M.T., & Meyer, M. Selective enrichment of damaged DNA molecules for ancient
830 genome sequencing. *Genome Res.* **24**, 1543-1549 (2014).
- 831 60. Meyer, M., et al., A high-coverage genome sequence from an archaic Denisovan individual.
832 *Science.* **338**, 222-226 (2012).
- 833 61. Maricic, T., Whitten, M., & Pääbo, S. Multiplexed DNA sequence capture of mitochondrial
834 genomes using PCR products. *PLoS One* **5**, e14004 (2010).
- 835 62. Rohland, N., & Hofreiter, M. Ancient DNA extraction from bones and teeth. *Nat. Protoc.* **2**,
836 1756–1762 (2007).
- 837 63. Meyer, M., & Kircher, M. Illumina sequencing library preparation for highly multiplexed
838 target capture and sequencing. *Cold Spring Harb. Protoc.* **6**, pdb.prot5448 (2010).
- 839 64. Fernandes, D.M., et al. The spread of steppe and Iranian-related ancestry in the islands of the
840 western Mediterranean. *Nat Ecol Evol.* **4**, 334-345 (2020).
- 841 65. John, J. S. SeqPrep, <https://github.com/jstjohn/SeqPrep> (2011).
- 842 66. Behar, D.M., et al. A "Copernican" reassessment of the human mitochondrial DNA tree from
843 its root. *Am J Hum Genet.* **90**, 675-84 (2012). Erratum in: *Am J Hum Genet.* **90**, 936 (2012).
- 844 67. Li, H., & Durbin, R. Fast and accurate short read alignment with Burrows–Wheeler transform.
845 *Bioinformatics*, **25**, 1754-1760 (2009).
- 846 68. Weissensteiner, H., et al. HaploGrep 2: mitochondrial haplogroup classification in the era of
847 high-throughput sequencing. *Nucleic Acids Res.* **44**, W58–W63 (2016).
- 848 69. Renaud, G., Stenzel, U., & Kelso, J. leeHom: adaptor trimming and merging for Illumina
849 sequencing reads. *Nucleic Acids Res.* **42**, e141 (2014).
- 850 70. Peltzer, A., et al. EAGER: efficient ancient genome reconstruction. *Genome Biol.* **17**, 60
851 (2016).
- 852 71. Kennett, D. J. et al. Archaeogenomic evidence reveals prehistoric matrilineal dynasty. *Nat.*
853 *Commun.* **8**, 14115 (2017).
- 854 72. Lohse, J. C., Madsen, D. B., Culleton, B. J. & Kennett, D. J. Isotope paleoecology of episodic
855 mid-to-late Holocene bison population expansions in the southern Plains, U.S.A. *Quat. Sci.*
856 *Rev.* **102**, 14–26 (2014).
- 857 73. Reimer, P. J. et al. IntCal13 and Marine13 radiocarbon age calibration curves 0–50,000 years
858 cal BP. *Radiocarbon* **55**, 1869–1887 (2013).
- 859 74. Bronk Ramsey, C. Bayesian analysis of radiocarbon dates. *Radiocarbon*, **51**, 337-360 (2009).
- 860 75. Rasmussen, M., et al. An Aboriginal Australian Genome Reveals Separate Human Dispersals
861 into Asia. *Science* **334**, 94–98 (2011).
- 862 76. Alexander, D. H., Novembre, J., & Lange, K. Fast model-based estimation of ancestry in
863 unrelated individuals. *Genome Res.* **19**, 1655-1664 (2009).

- 864 77. Chang, C., et al. Second-generation PLINK: rising to the challenge of larger and richer
865 datasets. *GigaScience* **4**, 7 (2015).
- 866 78. Busing, F. T. A., Meijer, E., & Leeden, R. Delete-m Jackknife for Unequal m. *Statistics and*
867 *Computing* **9**, 3-8 (1999).
- 868 79. Mallick, S.M., et al. The Simons Genome Diversity Project: 300 genomes from 142 diverse
869 populations, *Nature* **538**, 201-206 (2016).
- 870 80. Monroy, K.J.M., Jakobsson, M., & Günther, T. Estimating genetic kin relationships in
871 prehistoric populations. *PLoS One* **13**, e0195491 (2018).
- 872 81. Kennett, D.J., et al. Archaeogenomic evidence reveals prehistoric matrilineal dynasty. *Nat.*
873 *Commun.* **8**, 14115 (2017).

874

875 **Acknowledgements**

876 We thank David Anthony, Ofer Bar-Yosef, Katherine Brunson, Rowan Flad, Pavel
877 Flegontov, Qiaomei Fu, Wolfgang Haak, Iosif Lazaridis, Mark Lipson, Iain
878 Mathieson, Richard Meadow, Inigo Olalde, Nick Patterson, Pontus Skoglund, and
879 Dan Xu for valuable conversations and critical comments. We thank Naruya Saitou
880 and the Asian DNA Repository Consortium for sharing genotype data from present-
881 day Japanese groups. We thank Toyohiro Nishimoto and Takashi Fujisawa from the
882 Reibun Town Board of Education for providing the Funadomari Jomon samples, and
883 Hideyo Tanaka and Watru Nagahara from the Archeological Center of Chiba City
884 who are excavators of the Rokutsu Jomon site. The excavations at Boisman-2 site
885 (Boisman culture), the Pospelovo-1 site (Yankovsky culture), and the Roshino-4 site
886 (Heishui Mohe culture) were funded by the Far Eastern Federal University and the
887 Institute of History Far Eastern Branch of the Russian Academu of Sciences,
888 researches Pospelovo-1 funded by RFBR project number 18-09-40101. C.C.W was
889 funded by the Max Planck Society, the National Natural Science Foundation of China
890 (NSFC 31801040), the Nanqiang Outstanding Young Talents Program of Xiamen
891 University (X2123302), and Fundamental Research Funds for the Central Universities
892 (ZK1144). O.B. and Y.B. were funded by Russian Scientific Foundation grant 17-14-
893 01345. H.M. was supported by the grant JSPS 16H02527. The research of M.R. and
894 C.C.W has received funding from the European Research Council (ERC) under the
895 European Union's Horizon 2020 research and innovation programme (grant
896 agreement No 646612) granted to M.R. The research of C.S. is supported by the
897 Calleva Foundation and the Human Origins Research Fund. H.L was funded NSFC
898 (91731303, 31671297), B&R International Joint Laboratory of Eurasian

899 Anthropology (18490750300). J.K. was funded by DFG grant KR 4015/1-1, the
900 Baden Württemberg Foundation, and the Max Planck Institute. Accelerator Mass
901 Spectrometry radiocarbon dating work was supported by the National Science
902 Foundation (BCS- 1460369) to D.J.K. and B.J.C). D.R. was funded by NSF
903 HOMINID grant BCS-1032255, NIH (NIGMS) grant GM100233, the Paul Allen
904 Foundation, the John Templeton Foundation grant 61220, and the Howard Hughes
905 Medical Institute.

906

907 **Author Contributions**

908 Conceptualization, C.-C.W., H.-Y.Y., A.N.P., H.M., A.M.K., L.J., H.L., J.K., R.P.,
909 and D.R.; Formal Analysis, C.-C.W., R.B., M.Ma., S.M., Z.Z., B.J.C, and D.R.;
910 Investigation, C.-C.W., K.Si., O.C., A.K., N.R., A.M.K., M.Ma., S.M., K.W., N.A.,
911 N.B., K.C., B.J.C, L.E., A.M.L., M.Mi., J.O., K.S., S.W., S.Y., F.Z., J.G., Q.D., L.K.,
912 Da.L, Do.L, R.L., W.C., R.S., L.-X.W., L.W., G.X., H.Y., M.Z., G.H., X.Y., R.H.,
913 S.S., D.J.K., L.J., H.L., J.K., R.P., and D.R.; Resources, H.-Y.Y., A.N.P., R.B., D.T.,
914 J.Z., Y.-C.L, J.-Y.L., M.Ma., S.M., Z.Z., R.C., C.-J. H., C.-C.S., Y.G.N., A.V.T.,
915 A.A.T., S.L., Z.-Y.S., X.-M.W., T.-L.Y., X.H., L.C., H.D., J.B., E.Mi., D.E., T.-O.I.,
916 E.My., H.K.-K., M.N., K.Sh., D.J.K., R.P., and D.R.; Data Curation, C.-C.W., K.Si.,
917 O.C., A.K., N.R., R.B., M.Ma., S.M., B.J.C, L.E., A.A.T., and D.R.; Writing, C.-
918 C.W., H.-Y.Y., A.N.P., H.M., A.K., and D.R.; Supervision, C.-C.W., H.-Q.Z., N.R.,
919 M.R., S.S., D.J.K., L.J., H.L., J.K., R.P., and D.R.

920

921 **Competing interests**

922 The authors declare no competing interests.

Figure Legends

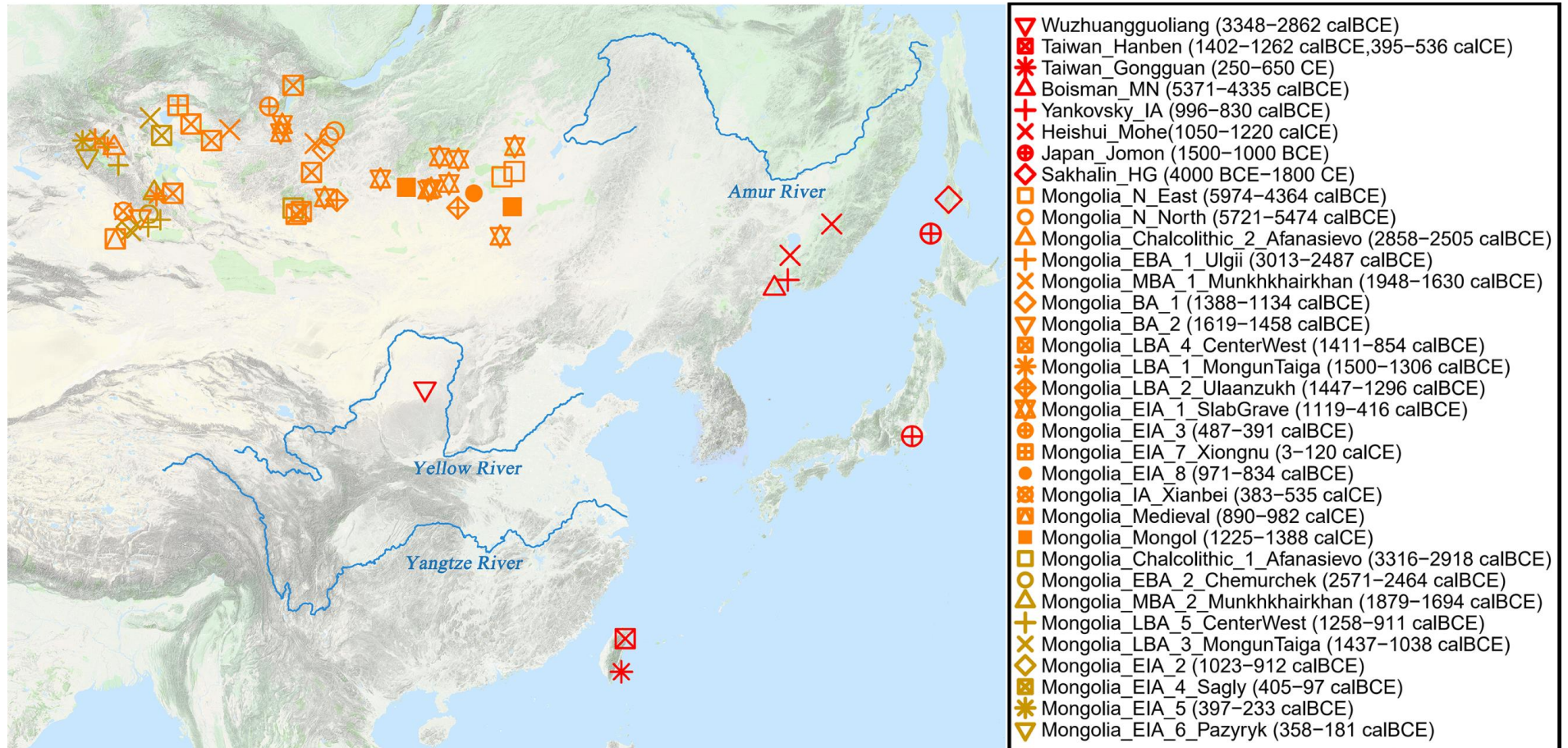


Figure 1: Geographical locations of newly reported ancient individuals. We use different colors for the two ancient Mongolia clusters. Detailed information are given in Table S1, Online Table 1 and Supplemental Experimental Procedures.

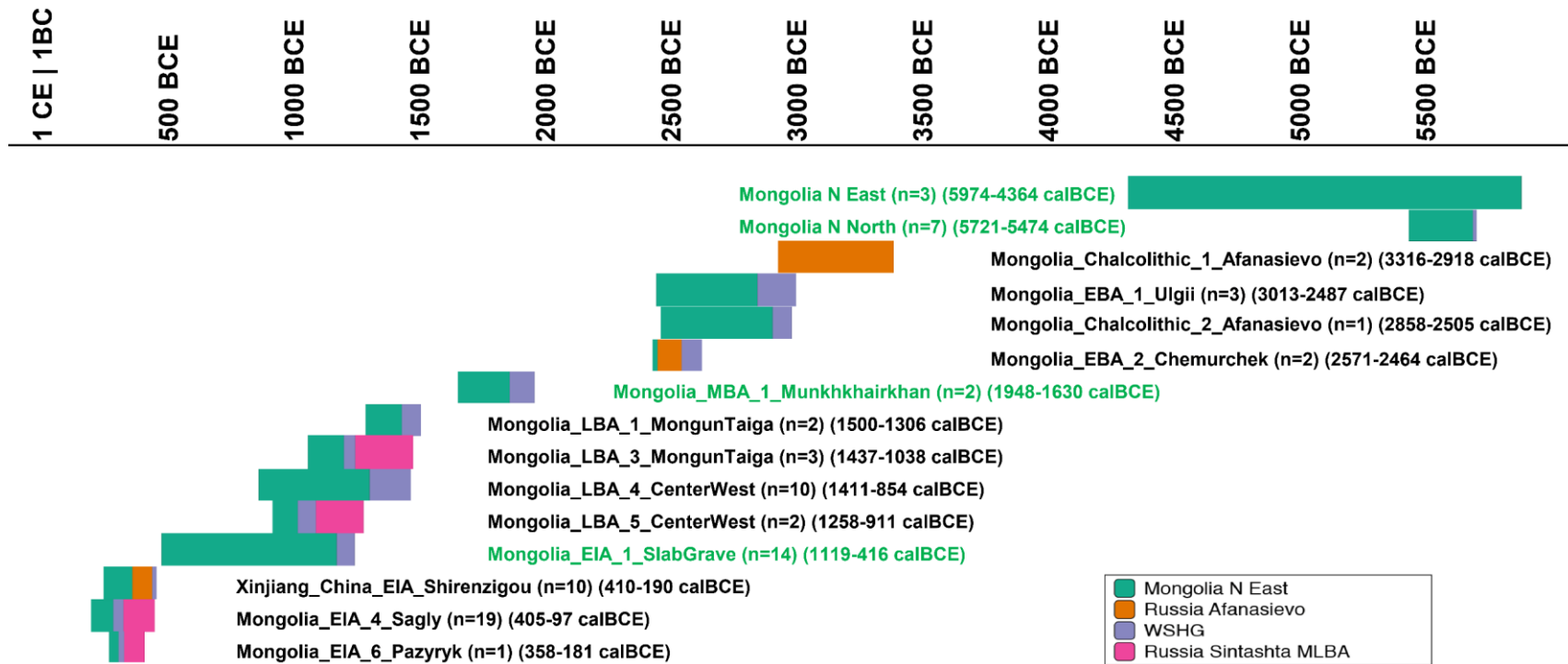


Figure 3: qpAdm modeling of ancestry change over time in Mongolia. We use Mongolia_East_N, Afanasievo, WSHG, and Sintashta_MLBA as sources, and for each combined archaeological and genetic grouping identify maximally parsimonious models (fewest numbers of sources) that fit with $P > 0.05$ (Online Table 5). We plot results for groupings that give a unique parsimonious model, and include at least one individual with data that “PASS” at high quality and with a confident chronological assignment (Online Table 1). The bars show proportions of each ancestry source, and we also include time spans for the individuals in the cluster. Groupings that include more eastern individuals (longitude > 102.7 degrees) are indicated in green and typically have very little Yamnaya-related admixture even at late dates.

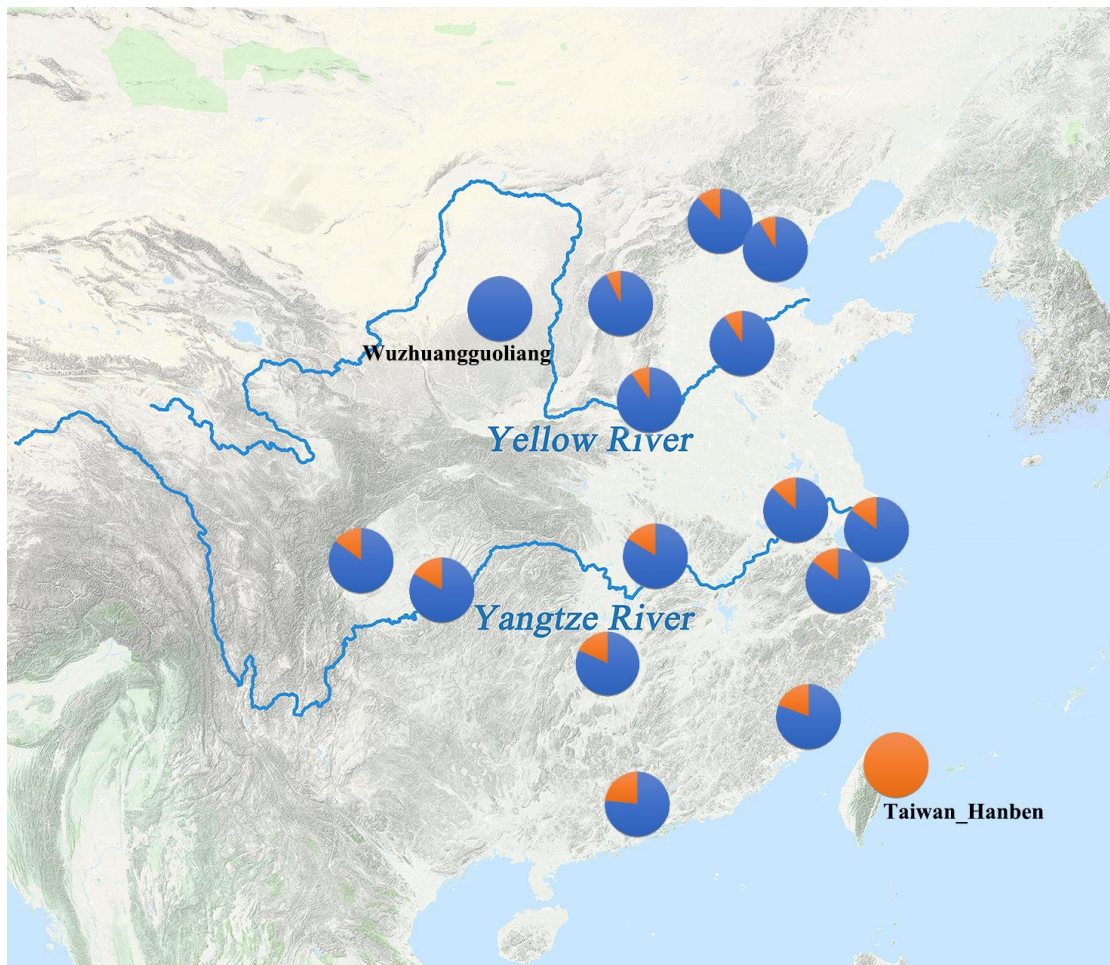


Figure 4: *qpAdm* modeling of Han Chinese cline. We used the ancient Wuzhuangguoliang as a proxy for Yellow River Farmers and Taiwan_Hanben as a proxy for Yangtze River Farmers related ancestry.

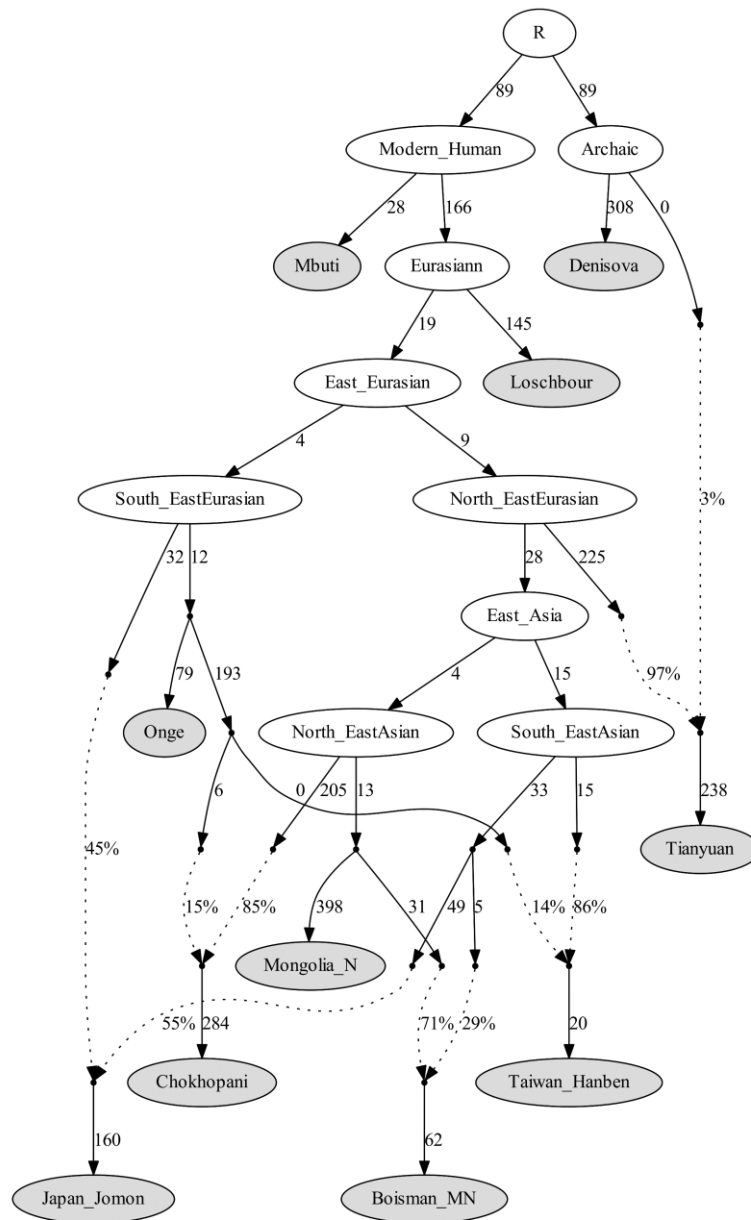


Figure 5: qpGraph modeling of a subset of East Asians. We used all available sites in the 1240K dataset, restricting to transversions only to replicate key results (Supplementary Information). We started with a skeleton tree that fits the data with Denisova, Mbuti, Onge, Tianyuan and Loschbour and one admixture event. We then grafted on Mongolia_East_N, Jomon, Taiwan_Hanben, Chokhopani, and Boisman in turn, adding them consecutively to all possible edges in the tree and retaining only graph solutions that provided no differences of $|Z| > 3$ between fitted and estimated statistics. We used the MSMC relative population split time to constrain models (the maximum discrepancy for this model is $|Z| = 2.8$). Drifts along edges are multiplied by 1000. Dashed lines represent admixture. Deep population splits are not well constrained due to a lack of data from Upper Paleolithic East Asians.

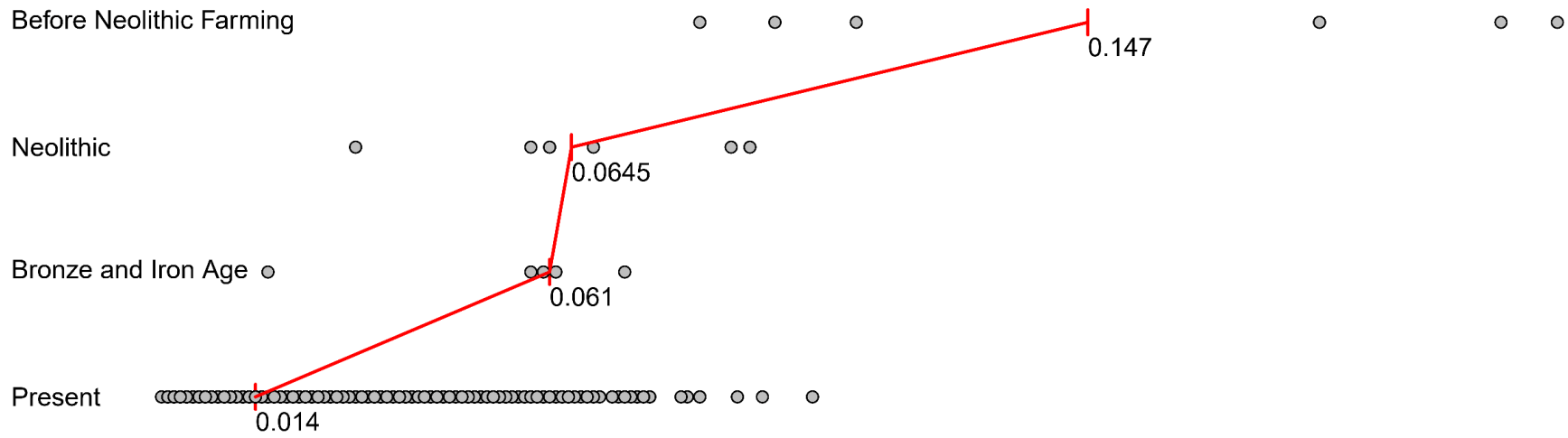


Figure 6. Homogenization of East Asian populations through mixture. Pairwise F_{ST} distribution among populations belonging to four time slices in East Asia; the median (red) of F_{ST} is shown.